


Crystal growth and magnetic anisotropy in the spin-chain ruthenate Na_2RuO_4

Ashiwini Balodhi and Yogesh Singh

Indian Institute of Science Education and Research (IISER) Mohali, Knowledge City, Sector 81, Mohali 140306, India

 (Received 19 June 2017; revised manuscript received 4 January 2018; published 12 February 2018)

We report single-crystal growth, electrical resistivity ρ , anisotropic magnetic susceptibility χ , and heat capacity C_p measurements on the one-dimensional spin-chain ruthenate Na_2RuO_4 . We observe variable range hopping (VRH) behavior in $\rho(T)$. The magnetic susceptibility with magnetic field perpendicular (χ_\perp) and parallel (χ_\parallel) to the spin chains is reported. The magnetic properties are anisotropic with $\chi_\perp > \chi_\parallel$ in the temperature range of measurements $T \approx 2\text{--}305$ K with $\chi_\perp/\chi_\parallel \approx 1.4$ at 305 K. From an analysis of the $\chi(T)$ data we attempt to estimate the anisotropy in the g factor and Van Vleck paramagnetic contribution. An anomaly in $\chi(T)$ and a corresponding step-like anomaly in C_p at $T_N = 37$ K confirms long-range antiferromagnetic ordering. This temperature is an order of magnitude smaller than the Weiss temperature $\theta \approx -250$ K and points to suppression of long-range magnetic order due to low dimensionality. A fit of the experimental $\chi(T)$ by a one-dimensional spin-chain model gave an estimate of the intrachain exchange interaction $2J \approx -85$ K and the magnitude of the interchain coupling $|2J_\perp| \approx 3$ K.

DOI: [10.1103/PhysRevMaterials.2.024403](https://doi.org/10.1103/PhysRevMaterials.2.024403)

I. INTRODUCTION

Study of low-dimensional magnets in the last few decades has led to the discovery of multiple quantum phases or systems. The quasi-one-dimensional antiferromagnetic chain material Sr_2CuO_3 [1,2], Haldane gap [3] in a $S = 1$ spin-chain compound $\text{Ni}(\text{C}_5\text{H}_{14}\text{N}_2)_2\text{N}_3(\text{PF}_6)$ [4], spin-Peierls transition in CeCuGe_3 [5], realization of the Shastry-Sutherland model in $\text{SrCu}_2(\text{BO}_3)_2$, high-temperature superconductivity in cuprates, and quantum spin-liquid state (QSL) in triangular lattice organic compounds $\kappa\text{-(BEDT-TTF)}_2\text{Cu}_2(\text{CN})_3$ [6,7] and in the kagome bilayer magnet $\text{Ca}_{10}\text{Cr}_7\text{O}_{28}$ [8] are just a few examples of the novel physics of low-dimensional magnets. Enhanced quantum fluctuations due to reduced dimensionality in these materials provides a rich playground for the study of quantum phases.

Recently, oxides with heavy transition metals ($4d, 5d$) have garnered much attention because of the possibility of novel magnetic behavior arising from strong spin-orbit coupling [9–11]. The square lattice iridate Sr_2IrO_4 has been studied extensively for its structural and magnetic similarities with the parent high- T_c cuprate material La_2CuO_4 [12–14]. The rare-earth pyrochlore iridate family $R_2\text{Ir}_2\text{O}_7$ has been studied for various novel behaviors, such as metal-insulator transitions [15] and possible topological properties [11,16–18]. Also, recently the two-dimensional Kitaev candidate materials $A_2\text{IrO}_3$ ($A = \text{Na}, \text{Li}$) [10,19,20] and $\alpha\text{-RuCl}_3$ [21,22], and the three-dimensional Kitaev materials $\gamma\text{-Li}_2\text{IrO}_3$ [23] and $\beta\text{-Li}_2\text{IrO}_3$ [24] have been studied for their novel magnetic properties and possible proximity to Kitaev's quantum spin liquid phase. Thus, there has been a resurgence in the interest in $4d$ - and $5d$ -based transition metal oxide (TMO) materials.

Additionally, whether a novel $J_{\text{eff}} = 1/2$ localized model or a quasimolecular orbital model is a more appropriate description for these compounds given their extended d shells is also under debate. The availability of single crystals of materials with heavy transition metal elements is therefore

of importance for advanced measurements such as x-ray absorption spectroscopy (XAS) or resonant inelastic x-ray scattering (RIXS), which help elucidate the electronic structure of the material.

In this work we focus on the $4d$ TMO linear-spin-chain compound Na_2RuO_4 , which combines low dimensionality and strong spin-orbit coupling. There have been some studies of the structural and magnetic properties of mostly polycrystalline Na_2RuO_4 [25–27]. X-ray and neutron diffraction studies have shown that the structure of Na_2RuO_4 is quasi-one-dimensional, with chains along the crystallographic b axis built up of corner-sharing RuO_5 trigonal bipyramids, where a Ru atom is surrounded by five oxygen atoms, making a linear one-dimensional spin-chain compound [25,26]. Na_2RuO_4 has also been reported to show an antiferromagnetic transition around $T_N = 37$ K [25–27]. The magnetic structure has been determined using neutron diffraction measurements. It was found that the Ru^{6+} magnetic moments are ordered antiferromagnetically along the chains (b axis), while the interchain interaction is ferromagnetic [26].

In this work we report a crystal growth method to obtain relatively large single crystals of Na_2RuO_4 . We also report electrical transport along the chain direction, anisotropic magnetic susceptibility and magnetization, and heat capacity measurements on these crystals.

II. EXPERIMENTAL DETAILS

Single crystals of Na_2RuO_4 were grown from off-stoichiometric mixtures of Na_2O_2 and RuO_2 in an oxidizing atmosphere. The high-purity starting materials Na_2O_2 (93% Alfa Aesar) and RuO_2 (99.99% Alfa Aesar) were taken in the ratio 1.5 : 1 and mixed thoroughly inside an inert gas glove box, pelletized, placed in an alumina crucible with a lid, and placed in a tube furnace. The tube was evacuated and filled with oxygen. The furnace was then heated to 750°C in 5 h and held

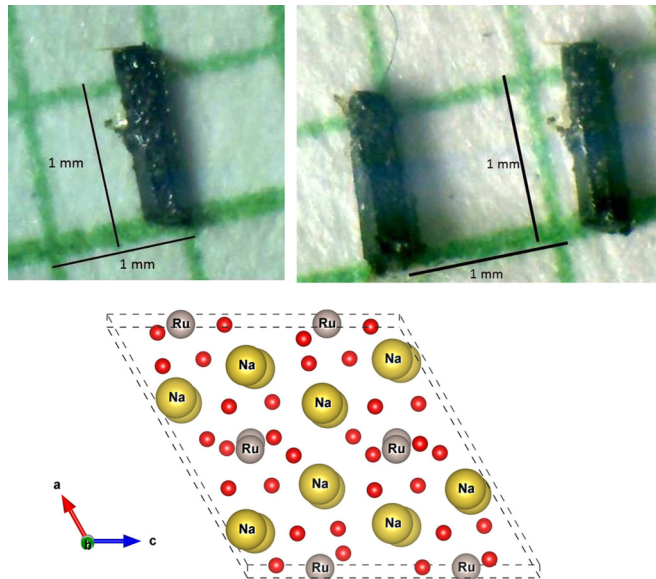


FIG. 1. (Top panel) Single crystals of Na_2RuO_4 on a millimeter grid. (Bottom panel) The crystal structure of Na_2RuO_4 viewed down the chain direction (crystallographic b axis).

there for 48 h followed by slow cooling ($3^\circ\text{C}-5^\circ\text{C}/\text{h}$) to room temperature. Shiny needlelike crystals with typical dimensions ($0.3 \times 1.3 \times 0.3$) mm, with the longest dimension being along the crystallographic b axis, were obtained buried in a polycrystalline matrix. Figure 1 shows a few typical crystals obtained in this way. The crystal structure shown in Fig. 1 was confirmed by single-crystal x-ray diffraction on a Bruker diffractometer. Single-crystal x-ray diffraction was used only to confirm the space group and cell parameters, which matched quite well with previously reported values. We therefore did not carry out a full refinement of the structure. The measurement gave the space group $P21/c$ and lattice parameters $a = 10.750 \text{ \AA}$, $b = 7.036 \text{ \AA}$, $c = 10.873 \text{ \AA}$, and $\beta = 119.18^\circ$, which are in excellent agreement with previously reported values [25,27]. Magnetic susceptibility, dc electrical transport, magnetization, and heat capacity measurements were done using a Quantum Design physical property measurement system (QD-PPMS).

III. RESULT AND DISCUSSION

A. Electrical transport

Figure 2 shows the electrical resistivity ρ versus temperature T measured between $T = 5 \text{ K}$ and $T = 300 \text{ K}$ for a crystal of Na_2RuO_4 with a current $I = 1 \text{ mA}$ along the crystallographic b axis. The electrical leads were made from $50\text{-}\mu\text{m}$ Pt wires and contacts were made using silver paint. The $\rho(T)$ shows insulating/semiconducting behavior in the whole temperature range. Inset I shows the data plotted as R versus $1/T$ on a semilog plot. From this plot it is clear that the data do not follow an Arrhenius kind of activated behavior in any extended temperature range. Inset II shows the data plotted as R versus $1/T^{1/4}$ on a semilog plot. Such behavior is expected when the conduction mechanism is variable range hopping (VRH) in three dimensions, which is usually observed in disordered semiconductors. It is clear that the $\rho(T)$ data

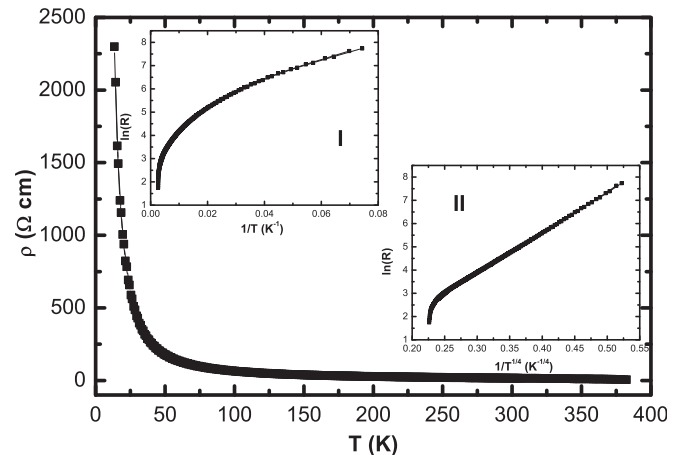


FIG. 2. Electrical resistivity ρ versus temperature T for currents along the b axis of Na_2RuO_4 . Inset I shows a semilog plot of R vs $1/T$ data. Inset II shows a semilog plot of R vs $1/T^{1/4}$.

for Na_2RuO_4 crystals have a temperature dependence which follows a VRH-like behavior over a large temperature range. The source of disorder in a high-quality crystal is unclear at the moment. However, we point out that several transition metal oxides based on $4d$ and $5d$ transition metals have recently been shown to follow such transport behavior. For example, transport on single crystals of Na_2IrO_3 [19] and single crystals of Sr_2IrO_4 have also been observed to follow a VRH behavior [28]. Therefore, a different common mechanism apart from disorder leading to this frequently observed behavior in the transport of transition metal oxides cannot be ruled out.

B. Magnetization and magnetic susceptibility

The magnetization M versus magnetic field H at different temperatures T both above and below the magnetic ordering temperature T_N is shown in Fig. 3. We observe that $M(H)$ is linear up to the highest magnetic fields $H = 9 \text{ T}$. The magnetic susceptibility $\chi = M/H$ measured with a magnetic field $H = 1 \text{ T}$ parallel (χ_{\parallel}) and perpendicular (χ_{\perp}) to the RuO_5 chains along the b axis are shown in Fig. 4(a). The powder average susceptibility defined for Na_2RuO_4 as $\chi_{\text{p-avg}} = 2\chi_{\perp} + \chi_{\parallel}$ was also calculated and is plotted for comparison in Fig. 4(a). The $\chi_{\text{p-avg}}$ so obtained is in good agreement with previous reports on polycrystalline samples [25–27].

From Fig. 4(a) the first thing to note is that $\chi_{\perp} > \chi_{\parallel}$ for all temperatures. This anisotropy most likely occurs due to a combination of single-ion anisotropy (since the point symmetry of Ru is D_{3h}), an anisotropic g factor, and/or a Van Vleck paramagnetic anisotropy in the material. The broad maximum around $T \approx 74 \text{ K}$ observed for both directions is the behavior typically observed for low-dimensional magnets and signals the onset of short-range magnetic order. At lower temperatures the χ decreases and there is a sharp cusp at $T_N = 37 \text{ K}$ observed for both directions, signaling the long-range magnetic ordering of Ru^{6+} ions. This can be seen in the Fig. 4 inset where the magnetic ordering for the two directions is indicated by arrows. This is consistent with previously reported data on polycrystalline samples [26,27]. A small upturn in magnetic susceptibility at the lowest temperatures suggests

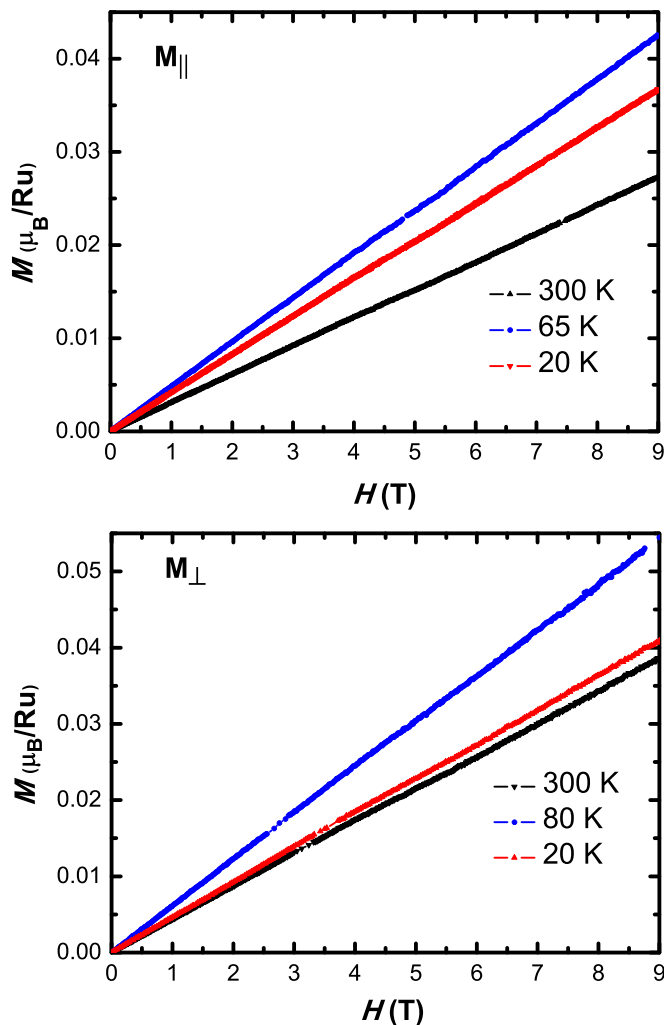


FIG. 3. Magnetization M versus magnetic field H at various temperatures T for Na_2RuO_4 single crystals with magnetic field H parallel M_{\parallel} (top panel) or perpendicular M_{\perp} (lower panel) to the spin-chain direction (crystallographic b -axis).

some Curie-like paramagnetic contribution most likely arising from impurities or unpaired spins.

From the $\chi(T)$ data we see that for both field directions as we cool from $T = 300$ K the data shows an upward curvature, and below about $T = 150$ K the data change behavior and curves downwards. Therefore, for $T \geq 200$ K we believe that we are in the high- T paramagnetic regime where a Curie-Weiss analysis can be used. The $\chi(T)$ data above $T = 220$ K for both directions were fit by a modified Curie-Weiss expression $\chi = \chi_0 + C/(T - \theta)$, with the temperature-independent contribution χ_0 , the Curie constant C , and Weiss temperature θ as fit parameters. It was found that the parameters χ_0 , which arise from a combination of core diamagnetism (isotropic) and Van Vleck paramagnetism (anisotropic), and C , which will be anisotropic due to g -factor anisotropy, could not be varied simultaneously to get unique values for these two fit parameters. In the fits we therefore fixed C to the value expected for $S = 1$ with a g factor $g = 2$. The fits for both field directions are shown as the solid curve through the $1/\chi(T)$ data shown in Fig. 4(b), and the values of χ_0 and θ obtained

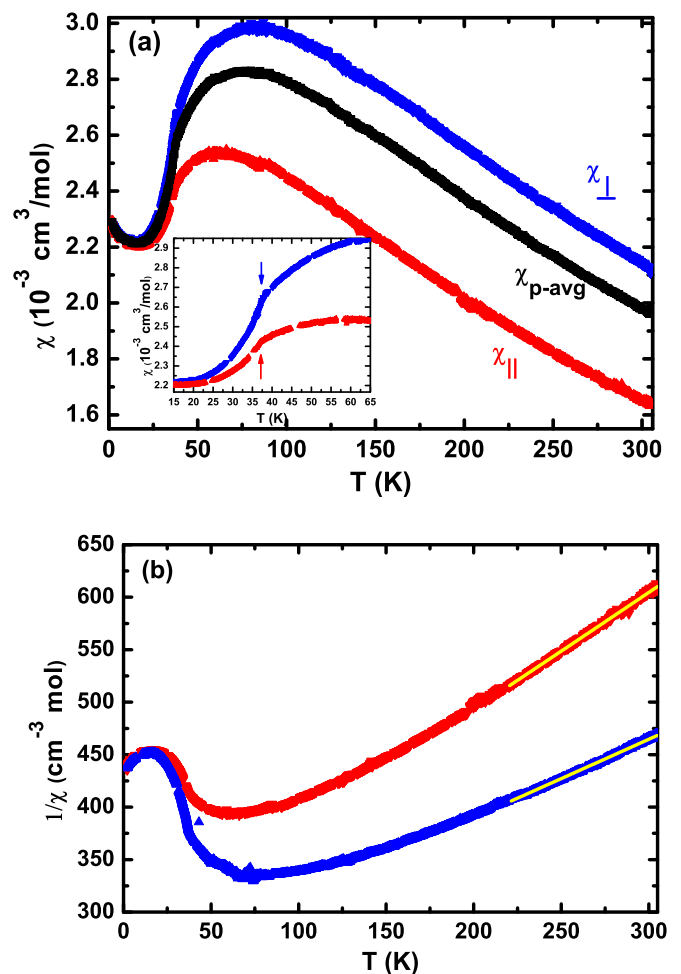


FIG. 4. (a) Magnetic susceptibility χ versus temperature T for Na_2RuO_4 single crystals with magnetic field $H = 1$ T applied parallel χ_{\parallel} or perpendicular χ_{\perp} to the spin-chain direction (crystallographic b axis). Inset shows the $\chi(T)$ data below $T = 65$ K to highlight the antiferromagnetic transition marked by arrows at $T_N = 37$ K for both directions. (b) $1/\chi(T)$ data for both field directions. The solid curve through the data at high temperatures is a fit by the modified Curie-Weiss expression given in the text. (c) χ_{\parallel} and χ_{\perp} data along with fits (solid curves) to a one-dimensional spin-chain model (see text for details).

from the fits are given in Table I. These results show that the Van Vleck paramagnetic contribution is an order of magnitude different for the two orientations. Since anisotropy in the Van Vleck contribution is linked to a g -factor anisotropy, it is most likely true that the g factor itself is highly anisotropic between the two directions. We, however, cannot find the anisotropy in both quantities simultaneously from our fits. Additionally,

TABLE I. Parameters obtained by fitting anisotropic magnetic susceptibility of Na_2RuO_4 .

| Alignment | χ_0 (cm^3/mol) | θ (K) |
|--------------------|---------------------------------------|--------------|
| χ_{\parallel} | $1.08(2) \times 10^{-5}$ | $-271(1)$ |
| χ_{\perp} | $3.03(3) \times 10^{-4}$ | $-242(1)$ |

the contribution of single-ion anisotropy due to the D_{3h} point symmetry of Ru cannot be determined uniquely from $\chi(T)$ measurements.

The Weiss temperatures θ were found to be similar for χ_{\parallel} and χ_{\perp} , respectively. These θ values are large and negative, indicating strong antiferromagnetic exchange interactions between the $S = 1$ moments. The observed magnetic ordering occurs at $T_N = 37$ K, which is an order of magnitude smaller than $|\theta|$, indicating strong low dimensionality which suppresses the long-range ordering to much lower temperatures.

To further explore the effect of low dimensionality on the magnetism, we have attempted to fit our $\chi(T)$ data by some models for quasi-one-dimensional magnetism. First we tried fitting our data by a phenomenological expression for the magnetic susceptibility of the $S = 1$ Haldane spin chain [29]:

$$\chi(T) = \chi_0 + \frac{0.125}{T} \exp\left(-\frac{0.451J}{T}\right) + \frac{0.564}{T} \exp\left(-\frac{1.793J}{T}\right),$$

where χ_0 is a T -independent term and J is the magnitude of the exchange interactions between the $S = 1$ spins within the chains. Fits to χ_{\parallel} and χ_{\perp} data for $T \geq 50$ K were performed using the above expression and the best fits, shown as the solid curves through the data in Fig. 5(a), gave the value $J \approx 72$ K. It is evident that while the fit reproduces qualitatively the main features (high- T Curie-like behavior and a broad maximum) of the data, the quantitative match is not very good.

We also tried fitting our data to a classical infinite spin-chain model given by [30]

$$\chi(T) = \chi_0 + \frac{Ng^2\mu_B^2 S(S+1)}{3k_B T} \times \frac{1+u}{1-u},$$

where

$$u = \coth\left[\frac{2JS(S+1)}{k_B T}\right] - \frac{k_B T}{2JS(S+1)}.$$

The fits to χ_{\parallel} and χ_{\perp} are shown in Fig. 5(b) as the solid curves through the data and gave the values $g \approx 1.84$ and $2J \approx -90$ K (1.52 and -72 K) for χ_{\perp} (χ_{\parallel}) when χ_0 was fixed to the values given in Table I. This model clearly gives a much better description of the experimental $\chi(T)$ behavior. It is, however, evident that substantial interchain couplings need to be included in any modeling of the data and that a model of isolated chains is not sufficient to completely understand the magnetism in Na_2RuO_4 . The presence of substantial interchain couplings is already evidenced by the presence of long-range magnetic order below $T_N = 37$ K. One can make an estimate of the interchain coupling by using the expression [31]

$$|2J_{\perp}| = \frac{T_N}{1.28n[\ln(5.8|2J|/T_N)]^{1/2}},$$

where n is the number of nearest-neighbor chains. Using $T_N = 37$ K, $n = 6$, and $2J$ found above, we get $2J_{\perp} \approx 3$ K. These values of the intrachain and interchain exchange constants are similar to those previously obtained by fitting the $\chi(T)$ data for a polycrystalline sample [26].

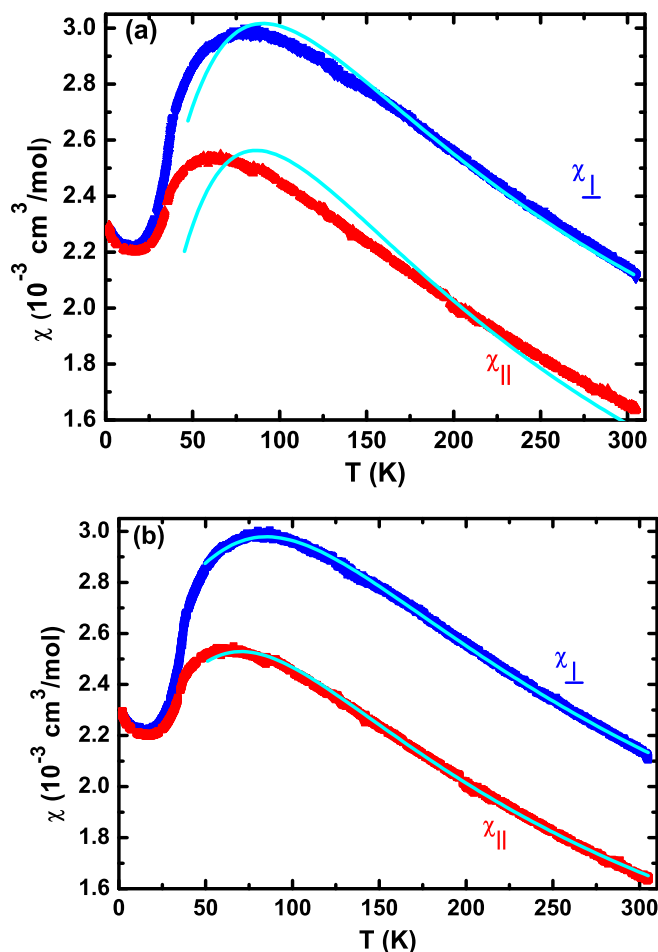


FIG. 5. The $\chi_{\perp}(T)$ and $\chi_{\parallel}(T)$ data fit by (a) the $S = 1$ Haldane spin chain model and (b) a classical infinite spin-chain model (see text for details).

C. Heat capacity

The heat capacity data in zero magnetic field is plotted in Fig. 6. The bulk nature of the long-range magnetic ordering in Na_2RuO_4 is confirmed by a sharp steplike anomaly at $T = 37$ K consistent with the magnetic susceptibility data presented above. The unavailability of an isostructural non-magnetic material which can be used as an approximate lattice contribution to the heat capacity for Na_2RuO_4 makes an analysis of magnetic entropy released at T_N difficult. However, we approximately estimate the size of the heat capacity anomaly at T_N by extrapolating the data above and below T_N to T_N . This gives ~ 8 J/mol K as the heat capacity jump at T_N . From mean-field theory, the jump at T_N for the ordering of $S = 1$ moments should be approximately $2R = 16.6$ J/mol K, where $R = 8.314$ J/mol K is the universal gas constant [32,33]. Thus the heat capacity jump is about half of what is expected within molecular field theory. This discrepancy can be attributed to the quasi-one-dimensional nature of the magnetism in Na_2RuO_4 , since some of the magnetic entropy has most likely already been removed above T_N by dynamic short-range ordering.

Heat capacity data below the ordering temperature can give information about the magnetic excitations. We attempted to fit the $C_p(T)$ data below T_N by various models. We tried a fit to

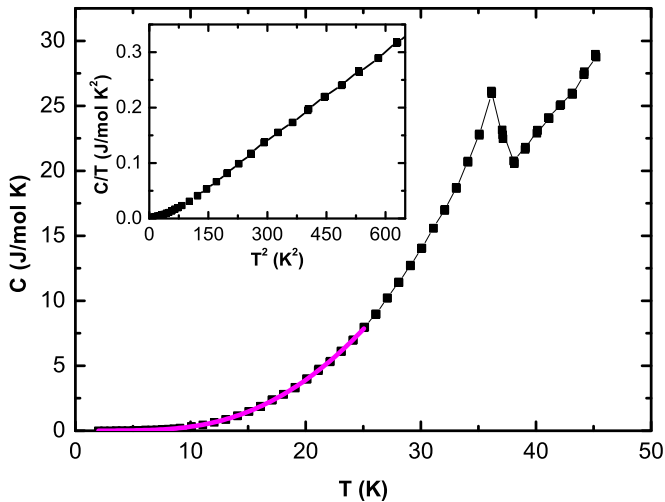


FIG. 6. Heat capacity C_p versus temperature for Na_2RuO_4 between $T = 2$ and 50 K. The inset shows the C/T vs T^2 data at low temperatures.

the data below $T = 20$ K by the expression $C_p = \beta_1 T + \beta_2 T^3$. Since Na_2RuO_4 is an insulator, the origin of the linear- T term in the heat capacity comes from the contribution of one-dimensional antiferromagnetic magnons. The T^3 term is the usual contribution from phonons plus possible contributions from three-dimensional antiferromagnetic magnons. The above expression gave a very poor fit to the data and the best fit gave a negative value for the prefactor of the linear- T term, which would be unphysical. The inset of Fig. 6 shows the C_p/T versus T^2 data inside the magnetically ordered state. It can be seen from this plot that the data at the lowest temperatures show a departure from the conventional $C_p \approx T^3$ behavior and falls more rapidly. We therefore attempted and were successful in getting an excellent fit to the following model with $C_p(T) = \beta T^3 + AT^{3/2} \exp^{-\Delta/T}$, where the second contribution is from a possible spin gap (the exponential) and the $T^{3/2}$ prefactor is from excitations of the ferromagnetically coupled chains. The fit is shown as the solid curve through the heat capacity data below $T = 25$ K in Fig. 6.

IV. CONCLUSION

In summary, we have presented a crystal growth method for obtaining sizable single crystals of the spin-chain ruthenate Na_2RuO_4 big enough for transport and anisotropic magnetic measurements. We have measured electrical transport with current along the chain direction, anisotropy in the magnetic

susceptibility, and heat capacity on these crystals. The electrical transport along the crystallographic b axis shows a variable range hopping behavior over a large temperature range. Although VRH behavior is usually associated with disorder and is observed in some doped semiconductors, we note that several $4d$ and $5d$ TMOs, including Sr_2IrO_4 and Na_2IrO_3 , have been reported to show such behavior. Anisotropy is clearly observed in magnetic measurements with $\chi_{\perp} > \chi_{\parallel}$. The origin of the magnetic anisotropy is most likely a combination of single-ion anisotropy, g -factor anisotropy, and anisotropy in the Van Vleck paramagnetic contribution. These effects cannot be separately extracted from current measurements. From an analysis of the $\chi(T)$ data we try to estimate the anisotropy arising from a combination of anisotropy in the g factors as well as in the Van Vleck paramagnetic contribution. The Weiss temperatures $\theta_{\parallel} = -271$ K and $\theta_{\perp} = -242$ K for the two field directions are large and antiferromagnetic. Both magnetic and heat capacity measurements confirm long-range antiferromagnetic order below $T_N = 37$ K. A suppression of T_N compared to θ by almost an order of magnitude most likely points to low dimensionality. We were able to obtain satisfactory fits to our $\chi(T)$ data to a model of a classical infinite chain of isolated $S = 1$ spins. These fits gave the intrachain exchange coupling $2J \approx -85$ K and the interchain exchange coupling $|2J_{\perp}| \approx 3$ K. Heat capacity data confirm bulk magnetic ordering at $T_N \approx 37$ K with a steplike anomaly which looks like a mean-field transition. The heat capacity jump at T_N is roughly half of the magnitude expected from a mean-field model for the ordering of $S = 1$ moments. This again indicates low-dimensional magnetic behavior, with a large fraction of the total magnetic entropy being recovered in short-range magnetic ordering above T_N . Heat capacity data in the magnetically ordered state could not be fit using a model of one-dimensional magnons and phonons. This is somewhat surprising given that Na_2RuO_4 is a fairly good example of a quasi-one-dimensional spin-chain magnet with large intrachain interactions but a much smaller ordering temperature.

Future measurements like electron spin resonance (ESR) and nuclear magnetic resonance (NMR) would be useful to get accurate estimates of the anisotropic g factor and the Van Vleck term in the susceptibility.

ACKNOWLEDGMENTS

We thank the x-ray facility at IISER Mohali. Y.S. acknowledges DST, India, for support through Ramanujan Grant No. SR/S2/RJN-76/2010 and through DST Grant No. SB/S2/CMP-001/20.

- [1] J. Schlappa, K. Wohlfeld, K. J. Zhou, M. Mourigal, M. W. Haverkort, V. N. Strocov, L. Hozoi, C. Monney, S. Nishimoto, S. Singh *et al.*, *Nature (London)* **485**, 82 (2012).
- [2] N. Motoyama, H. Eisaki, and S. Uchida, *Phys. Rev. Lett.* **76**, 3212 (1996).
- [3] F. D. M. Haldane, *Phys. Rev. Lett.* **50**, 1153 (1983).
- [4] Z. Honda, H. Asakawa, and K. Katsumata, *Phys. Rev. Lett.* **81**, 2566 (1998).

- [5] M. Hase, I. Terasaki, and K. Uchinokura, *Phys. Rev. Lett.* **70**, 3651 (1993).
- [6] S. Yamashita, Y. Nakazawa, M. Oguni, Y. Oshima, H. Nojiri, Y. Shimizu, K. Miyagawa, and K. Kanoda, *Nat. Phys.* **4**, 459 (2008).
- [7] M. Yamashita, N. Nakata, Y. Kasahara, T. Sasaki, N. Yoneyama, N. Kobayashi, S. Fujimoto, T. Shibauchi, and Y. Matsuda, *Nat. Phys.* **5**, 44 (2009).

- [8] C. Balz, B. Lake, J. Reuther, H. Luetkens, R. Schönemann, T. Herrmannsdörfer, Y. Singh, A. T. M. Nazmul Islam, E. M. Wheeler, J. A. Rodriguez-Rivera *et al.*, *Nat. Phys.* **12**, 942 (2016).
- [9] G. Jackeli and G. Khaliullin, *Phys. Rev. Lett.* **102**, 017205 (2009).
- [10] J. Chaloupka, G. Jackeli, and G. Khaliullin, *Phys. Rev. Lett.* **105**, 027204 (2010).
- [11] D. A. Pesin and L. Balents, *Nat. Phys.* **6**, 376 (2010).
- [12] M. K. Crawford, M. A. Subramanian, R. L. Harlow, J. A. Fernandez-Baca, Z. R. Wang, and D. C. Johnston, *Phys. Rev. B* **49**, 9198 (1994).
- [13] J. Kim, D. Casa, M. H. Upton, T. Gog, Y.-J. Kim, J. F. Mitchell, M. van Veenendaal, M. Daghofer, J. van den Brink, G. Khaliullin, and B. J. Kim, *Phys. Rev. Lett.* **108**, 177003 (2012).
- [14] O. B. Korneta, T. Qi, S. Chikara, S. Parkin, L. E. De Long, P. Schlottmann, and G. Cao, *Phys. Rev. B* **82**, 115117 (2010).
- [15] K. Matsuhira, M. Wakeshima, R. Nakanishi, T. Yamada, A. Nakamura, W. Kawano, S. Takagi, and Y. Hinatsu, *J. Phys. Soc. Jpn.* **76**, 043706 (2007).
- [16] B.-J. Yang and Y. B. Kim, *Phys. Rev. B* **82**, 085111 (2010).
- [17] X. Wan, A. M. Turner, A. Vishwanath, and S. Y. Savrasov, *Phys. Rev. B* **83**, 205101 (2011).
- [18] H. Zhang, K. Haule, and D. Vanderbilt, *Phys. Rev. Lett.* **118**, 026404 (2017).
- [19] Y. Singh and P. Gegenwart, *Phys. Rev. B* **82**, 064412 (2010).
- [20] Y. Singh, S. Manni, J. Reuther, T. Berlijn, R. Thomale, W. Ku, S. Trebst, and P. Gegenwart, *Phys. Rev. Lett.* **108**, 127203 (2012).
- [21] K. W. Plumb, J. P. Clancy, L. J. Sandilands, V. V. Shankar, Y. F. Hu, K. S. Burch, Hae-Young Kee, and Young-June Kim, *Phys. Rev. B* **90**, 041112 (2014).
- [22] A. Banerjee, C. A. Bridges, J. Q. Yan, A. A. Aczel, L. Li, M. B. Stone, G. E. Granroth, M. D. Lumsden, Y. Yiu, J. Knolle, S. Bhattacharjee, D. L. Kovrizhin, R. Moessner, D. A. Tennant, D. G. Mandrus, and S. E. Nagler, *Nat. Mater.* **15**, 733 (2016).
- [23] K. A. Modic, T. E. Smidt, I. Kimchi, N. P. Breznay, A. Biffin, S. Choi, R. D. Johnson, R. Coldea, P. Watkins-Curry, G. T. McCandless, J. Y. Chan, F. Gandara, Z. Islam, A. Vishwanath, A. Shekhter, R. D. McDonald, and J. G. Analytis, *Nat. Commun.* **5**, 4203 (2014).
- [24] T. Takayama, A. Kato, R. Dinnebier, J. Nuss, H. Kono, L. S. I. Veiga, G. Fabbris, D. Haskel, and H. Takagi, *Phys. Rev. Lett.* **114**, 077202 (2015).
- [25] K. M. Mogare, K. Friese, W. Klein, and M. Jansen, *Z. Anorg. Allg. Chem.* **630**, 547 (2004).
- [26] K. M. Mogare, D. V. Sheptyakov, R. Bircher, H.-U. Güdel, and M. Jansen, *Eur. Phys. J. B* **52**, 371 (2006).
- [27] M. Shikano, R. K. Kremer, M. Ahrens, H.-J. Koo, M.-H. Whangbo, and J. Darriet, *Inorg. Chem.* **43**, 5 (2004).
- [28] J. G. Rau, E. K-H. Lee, and H-Y. Kee, *Annu. Rev. Condens. Matter Phys.* **7**, 195 (2016).
- [29] J. Souletie, M. Drillon, P. Rabu, and S. K. Pati, *Phys. Rev. B* **70**, 054410 (2004).
- [30] O. Kahn, *Molecular Magnetism* (VCH Publishers, New York, 1993).
- [31] A. N. Vasiliev, O. L. Ignatchik, M. Isobe, and Y. Ueda, *Phys. Rev. B* **70**, 132415 (2004).
- [32] J. Fernández Rodríguez and J. A. Blanco, *Phys. Scr.* **71**, CC19, (2005).
- [33] H. E. Stanley, *Introduction to the Phase Transitions and Critical Phenomena* (Clarendon, Oxford, 1971).